Taylor & Francis
Taylor & Francis Group

IETE Journal of Research

ISSN: (Print) (Online) Journal homepage: https://www.tandfonline.com/loi/tijr20

A Hybrid Algorithm for Urban LULC Change Detection for Building Smart-city by Using WorldView Images

Ramen Pal, Somnath Mukhopadhyay, Debasish Chakraborty & Ponnuthurai Nagaratnam Suganthan

IETE JOURNAL OF RESEARCH
https://doi.org/10.1080/03772063.2022.2163928

A Hybrid Algorithm for Urban LULC Change Detection for Building Smart-city by Using WorldView Images

Ramen Pal [1], Somnath Mukhopadhyay [1], Debasish Chakraborty [2] and Ponnuthurai Nagaratnam Suganthan [3]

[1]Department of Computer Science and Engineering, Assam University, Silchar, India; [2]RRSC-East, ISRO, Kolkata, India; [3]School of Electrical & Electronic Engineering, Nanyang Technological University, Singapore, Singapore

ABSTRACT
Technological advancement in smart cities can have adverse effects on the environment. Timely monitoring of smart cities to preserve environmental sustainability is a thrust area of research. It can be done by using change detection with multi-temporal satellite data. The success of these methods solely depends on the calibre of the backend image segmentation and Land-use Land-cover classification technique. The limitation of using cutting-edge classification algorithms is the availability of a proper dataset and identification of the edge structure of different LULC classes. In contrast, a segmentation algorithm cannot detect LULC classes automatically. In this research, we eliminated these shortcomings by considering a hybrid approach. We proposed a multi-class Support Vector Machine (SVM) and ISODATA-embedded large-scale change detection method. This method can automatically segment, detect, and perform LULC change analysis. We have considered the multi-sensor dataset of Barasat, West Bengal, India, obtained from the WorldView satellite sensor for the experimental study. The proposed method is validated concerning three different cutting-edge methods.

KEYWORDS
Change detection; ISODATA; Multi-class SVM; Smart city; VHR MS image

1. INTRODUCTION

A smart city is a high-tech, and advanced urban zone. This initiative aims to steer social and economic growth to enhance humanity's quality of life. Nevertheless, it can lead to negative impacts on the environment. So, the environment's sustainability needs to be monitored timely to take preventive measures. We should monitor the changes between different LULC classes in a smart city from time to time. We can detect and quantify different changes in a smart city by using change detection methods. It is a procedure to analyze changes in different LULC classes of the earth's surface by using multi-temporal images taken from satellite or airborne imaging sensors. It becomes challenging if this analysis needs to be done on a large scale (using VHR Multi-spectral (MS) images). LULC defines the physical property and use of land. The success of LULC change detection [1], prediction [2], and identification [1] solely depends on the efficiency of the backhand segmentation or classification algorithm [3]. Classification algorithms are useful for detecting LULC classes automatically by avoiding any manual or ground-truthing operations [4–6]. However, these approaches cannot detect edge structures of different LULC classes. This limitation can be avoided using segmentation algorithms [7–10]. These algorithms to identify LULC classes automatically. A mixed approach can solve these issues. In this research, we proposed a multi-class Support Vector Machine (SVM) and ISODATA-embedded large-scale change detection method. It can automatically segment, detect, and perform change analysis.

In India, cities like Barasat having rapid technological growth in the last few decades. The rapid settlement, cropland, vegetation, and waterbody changes can be observed here. All LULC changes (waterbody to built-up, vegetation to built-up) must be promptly detected and quantified to implement preventive actions. It may limit the unwanted effect on the environment, flora, and fauna of Barasat and surrounding regions. We have considered very high-resolution panchromatic-sharpened images taken from the WorldView satellite sensor with a spatial resolution of 0.56 meters to quantify the changes in the last 10 years. We have analyzed the accuracy of our method by ground-truthing. We have visited the study area to note the actual LULC class occupied in 100 different locations for the image of the current year. We have taken the help of a handheld Ground Positioning System (GPS) device to serve this purpose. For the historical data, we have performed the ground-truthing by using

Google Earth Pro and ArcMap 10.5 Software. We have validated the performance of our proposed method concerning 3 different state-of-the-art methods. A brief literature survey on the state-of-the-art methods is presented in Section 2.

2. LITERATURE SURVEY

Proper selection of the change detection technique mostly depends on the targeted LULC feature (like vegetation, bare soil, water body, etc.) of the study area [11]. It is mainly because different statistical index functions are used for LULC classification [12]. In recent years many types of research have been reported in the literature that can efficiently minimize this dependency and apply it to solving change detection problems. In 2022, Saha *et al.* [13] presented a LULC change detection method by considering the Landsat dataset of an urban region of the sub-Himalayan area of north-east India. In this method, they have employed the Maximum Likelihood Classification (MLC) technique to classify multi-temporal (1991–2021) multi-spectral images of the study area. Then they predicted the changed map of the study area for the year 2050 using the Land Change Modeler (LCM) of the Multi-layer Perceptron Neural Network Markov Chain (MLPNN-MC) model. In 2022, Singh *et al.* [14] showed that classification techniques like Minimum Distance Classifier (MDC), Maximum Likelihood Classifier (MLC), and Spectral Angle Mapper (SAM) could efficiently classify multi-temporal MS datasets of Landsat-5 and Landsat-8. They have considered a semi-urban area of Imphal, India, as their study area. In 2016, Mousavirad *et al.* [10] proposed a meta-heuristic optimization algorithm-based satellite image segmentation method. They have considered the single objective variant of human mental search-based optimization. They have formulated their fitness function based on Kapur's and Otsu's entropy. In 2022, Pal *et al.* [15] proposed a new change detection method using a modified NSGA-II-based clustering algorithm. They have considered Intra-cluster and intra-cluster distance functions as their objective functions. In 2020, Xing *et al.* [8] proposed a clustering method based on a single objective emperor penguin optimization algorithm and Kapur's entropy function. In 2022, Mechkouri *et al.* [16] proposed a satellite image clustering algorithm based on the multi-objective optimization method. The fitness value of each solution is probabilistic. It is calculated by using Tsallis's and Rényi's entropic functions. In 2020, Alam *et al.* [17] proposed a LULC change detection method based on a Maximum Likelihood Classifier. They have quantified different LULC changes in Kashmir valley, India, from 1992–2015 using a dataset from the Landsat satellite sensor. In 2020, Mishra *et al.* [18] proposed a LULC change detection method using a Maximum Likelihood Classifier. They have considered a multi-temporal MS dataset obtained from a Landsat-5 satellite sensor to quantify changes in the Rani Khola Watershed, India.

The motivations and Contributions of our research are presented in Section 3.

3. MOTIVATION AND CONTRIBUTION

Based on the discussion in the previous section, the performance of a change detection algorithm solely depends on the underlying clustering or classification method. However, classification algorithms generally need to improve on the following: (i) the Unavailability of the dataset and (ii) the inability to detect edge structure properly. Whereas the clustering algorithm cannot identify LULC classes automatically. It motivated us to formulate an automatic method based on a hybrid approach. The contributions of this paper are as follows:

(1) A hybrid method for performing automatic segmentation and change analysis.
(2) Performing large-scale change analysis of Barasat, West Bengal, India, using very high-resolution satellite images.

In the rest of the paper: the proposed methodology is presented in Section 4, the result and analysis are presented in Section 5, and the conclusion and future scope are given in Sections 6 and 7, respectively.

4. PROPOSED METHODOLOGY

A graphical representation of the proposed method is presented in Figure 1.

It is a three-step process. In the first step, multi-temporal VHR MS images are segmented using the ISODATA clustering algorithm. Then entropy and variance information is extracted from the segmented image. In the next step, segmented clusters are mapped to the corresponding LULC class using the multi-class SVM classifier. It has constituted by using n number binary SVM classifier. In the present study, we have considered only 4 different LULC classes. So, the value for n is 4. SVM works on the following equation:

$$\frac{1}{2}z^T z + m \sum_{1}^{n} a_j \tag{1}$$

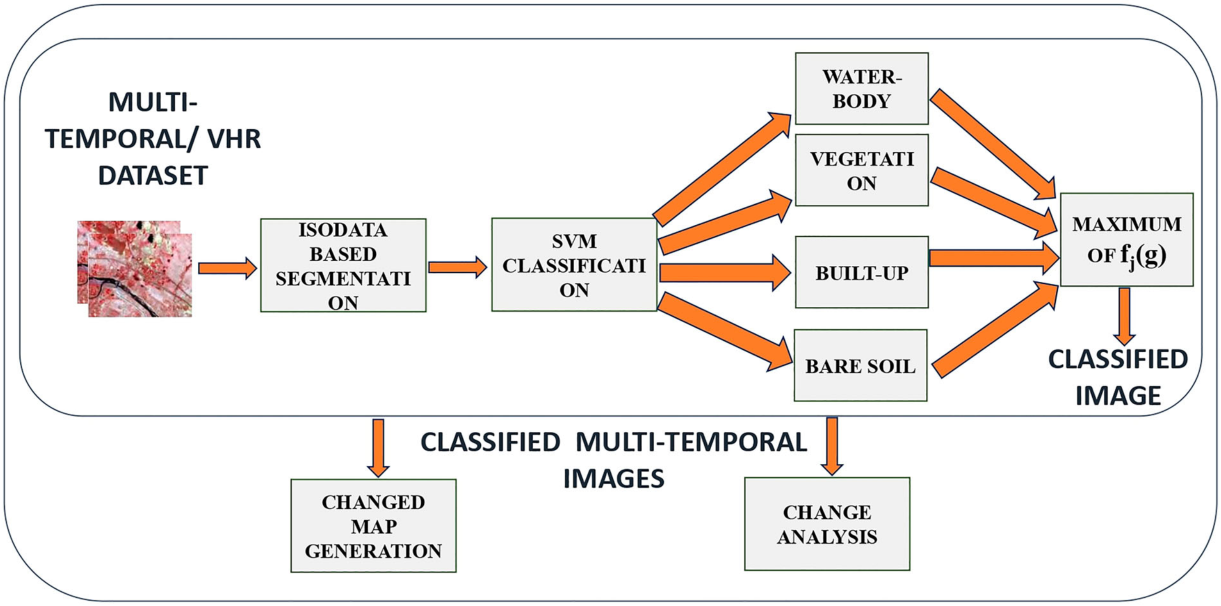

Figure 1: Proposed method for change detection

Subject to the constraints:

$$h_j(z^T \phi(g_j) + b) \geq 1-, \; \& \; a \geq 0, j = 1, 2, \ldots d \tag{2}$$

Here, d number of features are represented as $\langle g_j, h_j \rangle$ and $h_j \in \{+1, -1\}$. The labels for g_j denoted as $j = 1 \ldots d$. Optimization of weight are done by using Equation

$$\delta(z) = \frac{1}{2}||z||^2 + m \sum_{1}^{n} a_j \tag{3}$$

The bias value (b) is optimized by using Equation (4). It's a maximization function.

$$\Delta(\Lambda) = \sum_{1}^{d} \Lambda_j - \frac{1}{2} \sum_{j=1}^{d} \sum_{i=1}^{d} g_j h_i \Lambda_j \Lambda_i \kappa(g_j, g_i) \tag{4}$$

It works on the following conditions: $\Sigma_j^d h_j \Lambda_i = 0$ and $0 \geq \Lambda_j \leq r, \;\; j = 1 \ldots d$. Here, r is the regularization parameter. The support vectors define the decision function. It is a pair of g_j. We have considered the RBF kernel as the structure across all LULC classes' edges is non-linear. The RBF function is presented in Equation (5).

$$\kappa(g_j, g_i) = \phi(g_j)\dot{\phi}(g_i) = e^{-\beta|g_j - g_i|^2} \tag{5}$$

Here, weight is represented by using β. This classifier produced binary outputs in the form of $f_j(g)$, where $j \in [1, 4]$. Finally, the name of the LULC class is obtained by calculating the maximum value of $f_j(g)$. After that, parameters related to change analysis are quantified. In this process, the total area coverage for each class is calculated by multiplying the spatial resolution of the input image by the total number of pixels contained in each class. Then the partition matrices obtained after segmentation for a multi-temporal dataset are added to obtain the changed map. A multi-temporal dataset contains two images of the same scene. In contrast, the changing map represents the pixel-wise LULC transformation throughout the years.

5. RESULTS AND DISCUSSIONS

All the experimental validation of the proposed method concerning 3 different state-of-the-art methods (Mechkouri *et al.* [16], Xing *et al.* [8], and Mousavirad *et al.* [10]) are discussed in this section. We have considered the Gramin handheld GPS device to collect the ground truth information (reference points) for quantifying the classification accuracy.

5.1 Dataset

We have considered VHR and panchromatic-sharpened multi-temporal images of Barasat, India, taken from the WorldView satellite sensor. It is presented in Figure 2.

(a) Temporal Image-1 (b) Temporal Image-2

Figure 2: Experimental VHR image of Barasat, West Bengal, India, with a spatial resolution 0.46 meter, obtained from WorldView satellite sensors: (a) Temporal Image-1: Taken on 22nd February, 2011; (b) Temporal Image-2: Taken on 14th December, 2020

This dataset comprises two Geo-referenced images of the same location. The first image was taken on 22nd February 2011. The second one was taken on 14th December 2020. Both of these images have a spatial resolution of 0.46 meters.

5.2 Evaluation Metrics

The accuracy of the segmentation and change detection are quantified by using Overall Accuracy (OA) [19], Producer Accuracy (PA), Consumer Accuracy (CA) [19], Omission Error (OE) [19], Commission Error (CE) [19], and Kappa Co-efficient (K) [19].

5.3 Experimental Results

The result obtained after segmentation and LULC classification for the first temporal image (image of Barasat in 2011) is presented as the segmented map in Figure 3.

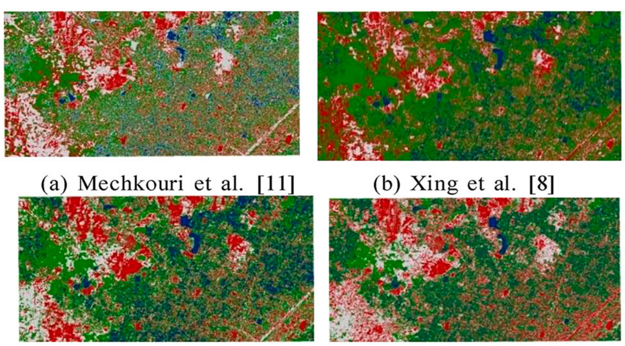

(a) Mechkouri et al. [11] (b) Xing et al. [8] (c) Mousavirad et al. [10] (d) Proposed Method

Figure 3: Segmented map obtained after segmenting the second temporal (2011) image of Barasat by using: (a) Mechkouri *et al.* [11], (b) Xing *et al.* [8], (c) Mousavirad *et al.* [10], and (d) Proposed method

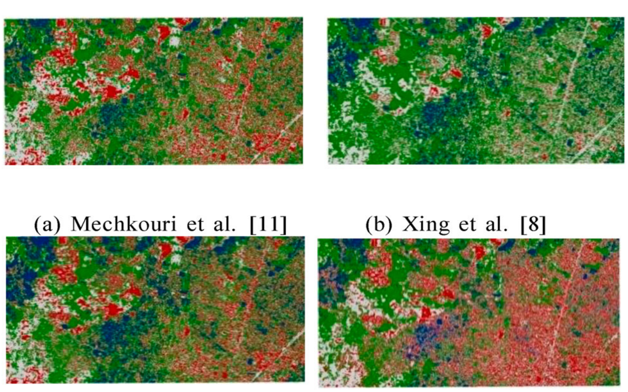

(a) Mechkouri et al. [11] (b) Xing et al. [8] (c) Mousavirad et al. [10] (d) Proposed Method

Figure 4: Segmented map obtained after segmenting the second temporal (2020) image of Barasat by using: (a) Mechkouri *et al.* [16], (b) Xing *et al.* [8], (c) Mousavirad *et al.* [10], and (d) Proposed method

Table 1: Performance comparison of the proposed method with different cutting edge techniques on the input dataset

Algorithm	Dataset	OA	PA	CA	K
Mechkouri *et al.* [16]	Temporal Image 1	78%	82%	83%	0.820
	Temporal Image 2	77.5%	79%	82.35%	0.806
Xing *et al.* [8]	Temporal Image 1	84%	85.8%	87.54%	0.842
	Temporal Image 2	83%	85%	86.71%	0.850
Mousavirad *et al.* [10]	Temporal Image 1	86.2%	87%	89%	0.884
	Temporal Image 2	85.5%	87.6%	88.2%	0.870
Proposed Method	Temporal Image 1	87.4%	88%	92%	0.90
	Temporal Image 2	86%	88.4%	90.6%	0.89

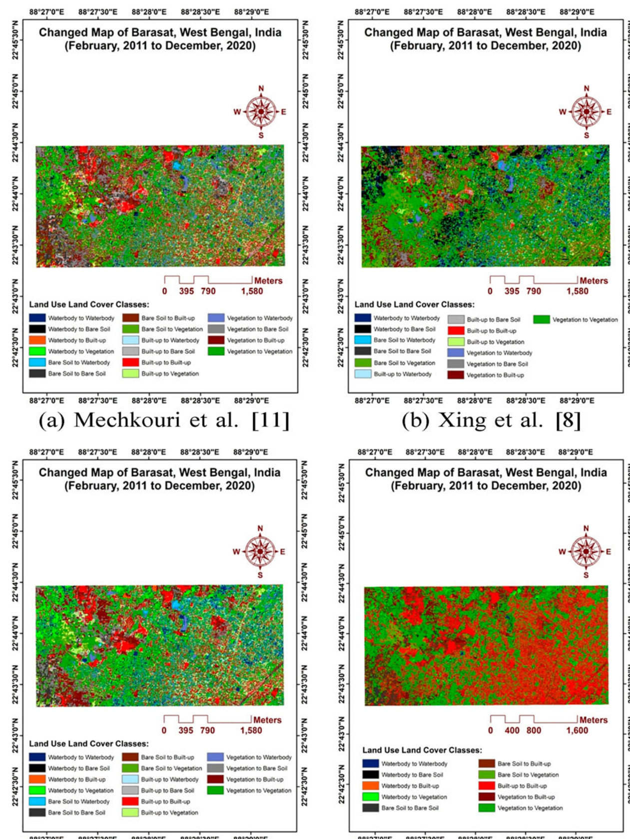

(a) Mechkouri et al. [11] (b) Xing et al. [8] (c) Mousavirad et al. [10] (d) Proposed Method

Figure 5: Changed map obtained for the multi – temporal (2011–2020) image of Barasat by using: (a) Mechkouri *et al.* [16], (b) Xing *et al.* [8], (c) Mousavirad *et al.* [10], and (d) Proposed method

The result obtained after segmentation and LULC classification for the second temporal image (image of Barasat in 2020) is presented as the segmented map in Figure 4.

Both of these images have 4 different LULC classes, namely, Waterbody (Blue), Vegetation (Green), Bare soil (Gray), and Built-up (Red). We can observe from these images that identifying different regions of LULC classes by the proposed method is better than others. The performance comparison of the proposed and cutting-edge

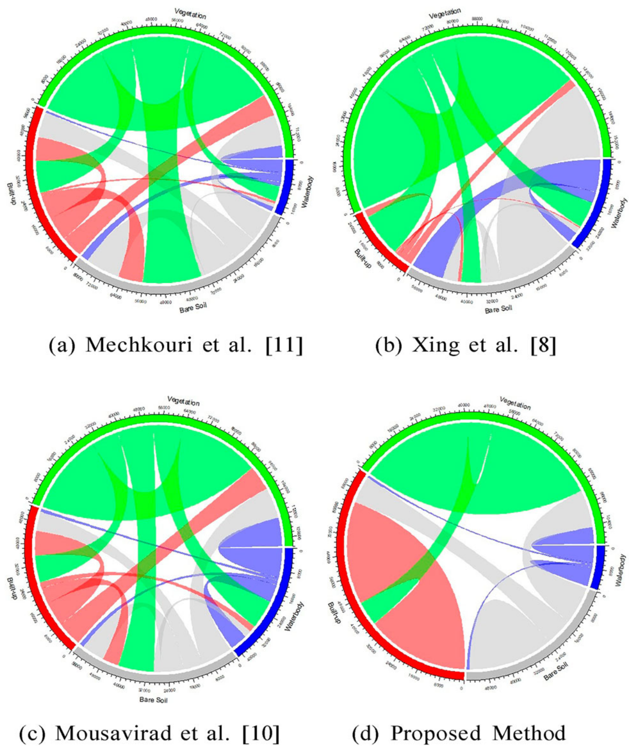

(a) Mechkouri et al. [11] (b) Xing et al. [8]

(c) Mousavirad et al. [10] (d) Proposed Method

Figure 6: Chord diagram representing the pixel-wise LULC transformation calculated by using: (a) Mechkouri *et al.* [16], (b) Xing *et al.* [8], (c) Mousavirad *et al.* [10], and (d) Proposed method

methods concerning accuracy are presented in Table 1 to support this claim.

Then changed map is generated for the duration of (2011–2020). It contains LULC class-wise changes throughout the years. It is presented in Figure 5.

We can observe that by using the method of Mechkouri *et al.* [16], Xing *et al.* [8], and Mousavirad *et al.*, some unusual LULC class changes are obtained. Changes like Built-up to Waterbody, Built-up to vegetation, and Vegetation to Waterbody are extracted. These changes cannot be observed in the input image. In contrast, these errors are eliminated by our proposed method. It can extract 10 different LULC changes that can be observed in the input image as well. LULC class changes are graphically presented in the form of a chord diagram presented in Figure 6. We can observe from this figure that in Barasat, changes like Waterbody to Vegetation (1.105899 KM^2), Waterbody to Built-up (3.796874 KM^2), Vegetation to Built-up (4.118573 KM^2) and Bare-soil to Built-up (3.270234 KM^2) are maximum.

We can observe from this figure that in Barasat, changes like Waterbody to Vegetation, Waterbody to Built-up, Vegetation to Built-up and Bare-soil to Built-up are maximum.

6. CONCLUSION

In recent years, the advancement of smart cities has led us to consider preserving the diversity of different LULC classes. We proposed a new approach to monitor these changes. By combining a segmentation and a classification algorithm, we have overcome the drawbacks of the most advanced change detection techniques. We no longer require training participants to rely on ground truth data. The WorldView satellite sensor's VHR satellite images have been taken into account. In every instance, with a good Kappa value, our proposed method outperformed three other state-of-the-art methodologies.

7. FUTURE SCOPE

The application of cutting-edge classification approaches is constrained by the lack of a suitable VHR dataset of smart cities. In the future, creating this type of information with airborne imaging sensors will allow us to create algorithms that are more effective.

DISCLOSURE STATEMENT

No potential conflict of interest was reported by the author(s).

ORCID

Ramen Pal http://orcid.org/0000-0002-0337-242X
Somnath Mukhopadhyay http://orcid.org/0000-0002-4532-6245
Debasish Chakraborty http://orcid.org/0000-0001-7170-1582
Ponnuthurai Nagaratnam Suganthan http://orcid.org/0000-0003-0901-5105

REFERENCES

1. R. V. Dey, Y. Zhang, and M. Zhong, "A review on image segmentation techniques with remote sensing perspective," in *Proceedings of the International Society for Photogrammetry and Remote Sensing Symposium (ISPR, S10)*, XXXVIII (Part 7A).

2. D. Zhang, M. M. Islam, and G. Lu, "A review on automatic image annotation techniques," *Pattern Recognit.*, Vol. 45, no. 1, pp. 346–62, 2012. doi:10.1016/j.patcog.2011.05.013.

3. P. Mitra, B. Uma Shankar, and S. K. Pal, "Segmentation of multispectral remote sensing images using active support vector machines," *Pattern Recognit. Lett.*, Vol. 25, no. 9, pp. 1067–74, 2004. doi:10.1016/j.patrec.2004.03.004.

4. K. Radhika, and S. Varadarajan, "A neural network based classification of satellite images for change detection applications," *Cogent Eng.*, Vol. 5, no. 1, pp. 1484587, 2018. doi:10.1080/23311916.2018.1484587.

5. J. Yan, L. Wang, W. Song, Y. Chen, X. Chen, and Z. Deng, “A time-series classification approach based on change detection for rapid land cover mapping,” *ISPRS. J. Photogramm. Remote. Sens.*, Vol. 158, pp. 249–62, 2019. 0924-2716. doi:10.1016/j.isprsjprs.2019.10.003.

6. T. H. G. Tran, C. Ressl, and N. Pfeifer, “Integrated change detection and classification in urban areas based on airborne laser scanning point clouds,” *Sensors*, Vol. 18, no. 2, p. 448, 2018. doi:10.3390/s18020448.

7. S. Suresh, and S. Lal, “An efficient cuckoo search algorithm based multilevel thresholding for segmentation of satellite images using different objective functions,” *Expert. Syst. Appl.*, Vol. 58, pp. 184–209, 2016. doi:10.1016/j.eswa.2016.03.032.

8. Z. Xing, “An improved emperor penguin optimization based multilevel thresholding for color image segmentation,” *Knowl. Based. Syst.*, Vol. 194, p. 105570, 2020. doi:10.1016/j.knosys.2020.105570. http://www.sciencedirect.com/science/article/pii/S0950705120300514.

9. Y. Li, S. Feng, X. Zhang, and L. Jiao, “SAR image segmentation based on quantum-inspired multi-objective evolutionary clustering algorithm,” *Inf. Process. Lett.*, Vol. 114, no. 6, pp. 287–93, 2014. doi:10.1016/j.ipl.2013.12.010.

10. S. J. Mousavirad, and H. Ebrahimpour-Komleh, “Human mental search-based multilevel thresholding for image segmentation,” *Appl. Soft. Comput.*, Vol. 97, pp. 105427, 2020. doi:10.1016/j.asoc.2019.04.002. http://www.sciencedirect.com/science/article/pii/S1568494619301838.

11. A. H. Chughtai, H. Abbasi, and I. R. Karas, “A review on change detection method and accuracy assessment for land use land cover,” *Remote Sens. Appl. Soc. Environ.*, Vol. 22, p. 100482, 2021. ISSN 2352-9385. doi:10.1016/j.rsase.2021.100482.

12. M. Weigand, J. Staab, M. Wurm, and H. Taubenböck, “Spatial and semantic effects of LUCAS samples on fully automated land use/land cover classification in high-resolution sentinel-2 data,” *Int. J. Appl. Earth Obs. Geoinf.*, Vol. 88, p. 102065, 2020. ISSN 1569-8432. doi:10.1016/j.jag.2020.102065.

13. P. Saha, R. Mitra, K. Chakraborty, and M. Roy, “Application of multi layer perceptron neural network Markov chain model for LULC change detection in the Sub-Himalayan North Bengal,” *Remote Sens. Appl. Soc. Environ.*, Vol. 26, p. 100730, 2022. ISSN 2352-9385. doi:10.1016/j.rsase.2022.100730.

14. K. T. Singh, N. M. Singh, and T. T. Devi, “A remote sensing, GIS based study on LULC change detection by different methods of classifiers on landsat data,” in *Innovative Trends in Hydrological and Environmental Systems. Lecture Notes in Civil Engineering*, Vol 234, A.K. Dikshit, B. Narasimhan, B. Kumar, and A.K. Patel, Eds. Singapore: Springer, 2022, pp. 107–17. doi:10.1007/978-981-19-0304-5_9

15. R. Pal, S. Mukhopadhyay, D. Chakraborty, and P. N. Suganthan, “Very high-resolution satellite image segmentation using variable-length multi-objective genetic clustering for multi-class change detection,” *J. King Saud Univ. – Comput. Inform. Sci.*, Vol. 34, pp. 9964–76, 2022. ISSN 1319-1578. doi:10.1016/j.jksuci.2021.12.023.

16. S. M. Mechkouri, S. El Joumani, R. Zennouhi, and L. Masmoudi, “Multi-objective optimization for worldview image segmentation funded on the entropies of tsallis and rényi,” *Multimed. Tools. Appl.*, Vol. 79, pp. 30637–52, 2020. doi:10.1007/s11042-020-09572-4.

17. A. Alam, M. S. Bhat, and M. Maheen, “Using landsat satellite data for assessing the land use and land cover change in Kashmir valley,” *GeoJournal*, Vol. 85, pp. 1529–43, 2020. doi:10.1007/s10708-019-10037-x.

18. P. K. Mishra, A. Rai, and S. C. Rai, “Land use and land cover change detection using geospatial techniques in the Sikkim Himalaya, India,” *Egyptian J. Remote Sens. Space Sci.*, Vol. 23, no. 2, pp. 133–43, 2020. ISSN 1110-9823. doi:10.1016/j.ejrs.2019.02.001.

19. L. Xu, W. Jing, H. Song, and G. Chen, “High-resolution remote sensing image change detection combined with pixel-level and object-level,” *IEEE. Access.*, Vol. 7, pp. 78909–18, 2019. doi:10.1109/ACCESS.2019.2922839.

AUTHORS

Ramen Pal received his BE degree in information technology at the University of Burdwan, Burdwan, India in 2015. He completed his MTech degree in computer science and engineering at the University of Kalyani, India in 2018. He is currently pursuing PhD at the Department of Computer Science and Engineering, Assam University, Silchar, India. His areas of interest are soft computing, multi-spectral image processing, urban change analysis, and portfolio optimization for stocks.

Email: ramen.pal673@gmail.com

Somnath Mukhopadhyay is currently an assistant professor at the department of computer science and engineering, Assam University, Silchar, India. He completed his MTech and PhD degrees in computer science and engineering at the University of Kalyani, India, in 2011 and 2015, respectively. His areas of interest are image processing, remote sensing, and soft computing.

Corresponding author. Email: som.cse@live.com

Debasish Chakraborty is the head applications at Regional Remote Sensing Centre – East (RRSC-East), National Remote Sensing Centre (NRSC), Indian Space Research Organization (ISRO). He has obtained PhD from Jadavpur University, Kolkata, India. His research interests include remote sensing, GIS, satellite image processing, machine learning and deep learning. He was honored with ISRO team excellence awards.

Email: deba.isro@gmail.com

Ponnuthurai Nagaratnam Suganthan (Fellow, IEEE) received the BA and MA degrees from the University of Cambridge, Cambridge, UK, and the PhD degree from Nanyang Technological University, Singapore. He was a recipient of the IEEE Transactions on Evolutionary Computation outstanding paper award in 2012, and the Highly cited researcher award by the Thomson Reuters in computer science in 2015. He is an Associate Editor of the IEEE Transactions on Evolutionary Computation, IEEE Transactions on Cybernetics, Information Sciences, and Pattern Recognition and the Founding Co-Editor-in-Chief of Swarm and Evolutionary Computation.

Email: epnsugan@ntu.edu.sg